Isotope Fractionation from In Vivo Methylmercury Detoxification in Waterbirds

Brett A Poulin, Sarah E Janssen, Tylor J Rosera, David P Krabbenhoft, Collin A Eagles-Smith, Joshua T Ackerman, A. Robin Robin Stewart, Eunhee Kim, Zofia Baumann, Jeong-Hoon Kim, et al.

Isotope Fractionation from *In Vivo* Methylmercury Detoxification in Waterbirds

Brett A. Poulin[a,b*], Sarah E. Janssen[c], Tylor J. Rosera[c,d], David P. Krabbenhoft[c], Collin A. Eagles-Smith[e], Joshua T. Ackerman[f], A. Robin Stewart[g], Eunhee Kim[h], Zofia Baumann[i], Jeong-Hoon Kim[j], and Alain Manceau[k*]

[a]Department of Environmental Toxicology, University of California Davis, Davis, CA 95616, USA (current address)
[b]U.S. Geological Survey, Water Mission Area, Boulder, Colorado 80303, United States
[c]U.S. Geological Survey, Upper Midwest Water Science Center, Middleton, Wisconsin 53562, United States
[d]Environmental Chemistry and Technology Program, University of Wisconsin-Madison, Madison, WI 53706, USA
[e]U.S. Geological Survey, Forest and Rangeland Ecosystem Science Center, Corvallis, Oregon, 97331, United States
[f]U.S. Geological Survey, Western Ecological Research Center, Dixon Field Station, Dixon, California, 95620, United States
[g]U.S. Geological Survey, Water Mission Area, Menlo Park, California, USA
[h]Citizens' Institute for Environmental Studies (CIES), Seoul, Korea
[i]Department of Marine Sciences, University of Connecticut, Groton, CT 06340, USA
[j]Division of Life Sciences, Korea Polar Research Institute, Incheon, Korea
[k]University Grenoble Alpes, ISTerre, CNRS, CS 40700, 38058 Grenoble, France
* Corresponding authors. Tel: +1 530 754 2454. *Email address:* bapoulin@ucdavis.edu (B.A. Poulin), alain.manceau@univ-grenoble-alpes.fr (A. Manceau)

Abstract

The robust application of stable mercury (Hg) isotopes for mercury source apportionment and risk assessment necessitates the understanding of mass-dependent fractionation (MDF) due to internal transformations within organisms. Here, we used high energy-resolution XANES spectroscopy and isotope ratios of total mercury (δ^{202}THg) and methylmercury (δ^{202}MeHg) to elucidate the chemical speciation of Hg and the resultant MDF due to internal MeHg demethylation in waterbirds. In three waterbirds (Clark's grebe, Forster's tern, south polar skua), between 17-86% of the MeHg was demethylated to inorganic mercury (iHg) species primarily in the liver and kidneys as Hg-tetraselenolate ($Hg(Sec)_4$) and minor Hg-dithiolate ($Hg(SR)_2$) complexes. Tissular differences between δ^{202}THg and δ^{202}MeHg correlated linearly with %iHg ($Hg(Sec)_4$ + $Hg(SR)_2$), and were interpreted to reflect a kinetic isotope effect during *in vivo* MeHg demethylation. The product-reactant isotopic enrichment factor ($\varepsilon_{p/r}$) for the demethylation of MeHg → $Hg(Sec)_4$ was −2.2 ± 0.1‰. δ^{202}MeHg values were unvarying within each bird regardless of $Hg(Sec)_4$ abundance, indicating fast internal cycling or replenishment of MeHg relative to demethylation. Our findings document a universal selenium-dependent demethylation

reaction in birds, provide new insights on the internal transformations and cycling of MeHg and $Hg(Sec)_4$, and allow for mathematical correction of $\delta^{202}THg$ values due to the MeHg → $Hg(Sec)_4$ reaction.

Keywords: Mercury, demethylation, isotopes, MDF, birds

Introduction

Mercury (Hg) is a neurotoxin that impacts the health of aquatic and terrestrial animals worldwide.[1] Higher trophic level organisms (e.g., birds, fish, mammals) are exposed to methylmercury (MeHg) through dietary sources, which is assimilated in the digestive tract, circulated in the bloodstream, and retained in the protein of tissues as a MeHg-cysteine complex (MeHg-Cys).[2–4] The toxicological risks of MeHg to aquatic and terrestrial organisms are governed by *in vivo* transformations, inter-tissular exchanges, and depuration rates and pathways of MeHg and other biologically-relevant forms of mercury.[1] In birds, MeHg can be demethylated in the liver,[5,6] depurated into feathers during molt or to offspring by maternal transfer,[7] and excreted.[1] Stable isotope ratios of mercury are a central tool for ecologic risk assessment and mercury source apportionment to organisms,[8–14] yet critical questions remain on the isotopic fractionation of mercury by *in vivo* transformations.

The *in vivo* demethylation of MeHg induces mass-dependent fractionation (MDF) of mercury isotopes (denoted by $\delta^{202}Hg$) as reported in birds,[6] fish,[15] and mammals.[9,16–18] The development[19,20] and application[16,17] of methods for species-specific mercury isotope ratio measurements show promise for determining the effect of *in vivo* transformations on mercury isotope ratios. However, a chief barrier is quantifying the chemical speciation of inorganic Hg (iHg) with high precision in natural tissues. High energy-resolution X-ray absorption near-edge structure (HR-XANES) spectroscopy can identify and quantify mixtures of biologically-relevant mercury species at sub-parts-per-million concentration.[3,4,21–23] Recent application of HR-XANES in terrestrial bird and freshwater fish tissues revealed that MeHg-Cys is detoxified to a Hg-tetraselenolate ($Hg(Sec)_4$) complex, likely by selenoprotein P (SelP).[4] $Hg(Sec)_4$ was shown to be the organic precursor to nanoparticulate HgSe,[4] which has been observed with $Hg(Sec)_4$ by HR-XANES in marine birds[22] and by normal resolution XANES in birds and mammals.[24–26] Linking the chemical speciation of iHg (that indicate specific internal reactions) and MDF of stable mercury isotopes is needed to inform on the internal transformations and trafficking of mercury.

Here, tissues and feathers of piscivorous waterbirds from lacustrine (Clark's grebe, *Aechmophorus clarkia*),[4,27] estuarine (Forster's tern, *Sterna forsteri forsteri*),[28] and marine (south polar skua, *Stercorarius maccormicki*) environments were measured for mercury speciation by HR-XANES spectroscopy and species-specific isotope ratios. Previous research indicates internal MeHg demethylation in these birds.[4,5] Study goals were to determine the product-reactant isotopic enrichment factor ($\varepsilon_{p/r}$) for the *in vivo* detoxification of MeHg to $Hg(Sec)_4$ and investigate the internal cycling of biologically-relevant mercury species. The findings are discussed in context of MeHg detoxification in vertebrates and implications of *in vivo* MDF of mercury isotopes on environmental isotope applications.

Materials and Methods

Biologic Tissues

Tissues and feathers from three birds were analyzed including a Clark's grebe (*A. clarkia*; adult male) from Lake Berryessa (California, USA; collected September 11, 2012), a Forster's tern (*S. forsteri forsteri*; adult female) from the south San Francisco Bay (California, USA; collected June 13, 2018), and a south polar skua (*S. maccormicki;* adult female) from Cape Hallett located in the northern Victoria Land coast of the Ross Sea (Antarctica; collected November 22, 2016). The Clark's grebe and Forster's tern were necropsied to obtain the following tissues: breast feather, brain, pectoral muscle, kidneys, and liver. The south polar skua was necropsied to obtain the muscle, kidneys, and liver. Tissues were lyophilized and homogenized. Clark's grebe tissues were analyzed previously for mercury speciation by HR-XANES and mercury and selenium association with selenoproteins.[4]

HR-XANES Measurements

HR-XANES spectra of the Clark's grebe tissues are published[4,29] and were measured identically during the same experimental session on the Forster's tern and south polar skua samples. The south polar skua kidney tissue was not measured by HR-XANES. Complete details are provided in the SI. Briefly, mercury L_3-edge HR-XANES spectra were measured on freeze-dried samples with high-reflectivity analyzer crystals[30] (beamline ID26, European Synchrotron Radiation Facility). Proportions of Hg were quantified using least-squares fitting of data with linear combinations of diverse reference spectra.[4,21,22] The reference spectrum of MeHg-Cys was represented using the Clark's grebe breast feather spectrum, which was suitable based on a spectral comparison to previously analyzed biological samples with exclusively MeHg-Cys.[4] The spectrum of $Hg(Sec)_4$ was determined by iterative transformation factor analysis.[4] The spectrum of Hg-dithiolate ($Hg(SR)_2$) complex in biota[3] was represented using Hg(L-glutathione)$_2$ at pH 7.4.[31,32]

Chemical and Isotope Analyses

Details on chemical and isotope measurements are provided in the SI. Briefly, tissues and feathers were measured for total mercury (THg), MeHg, and total selenium concentration.[33] Stable mercury isotope ratios were measured on THg acid digests[11,12] and resin separated MeHg fractions[20] of all samples from the Clark's grebe and Forster's tern. For the south polar skua, THg isotope ratios were measured on all tissues (muscle, kidneys, and liver) and on the MeHg fraction of the kidneys. Isotope analyses were performed using a multi-collector inductively coupled plasma mass spectrometer following established protocols[34,35] on material previously exposed to the X-ray beam for HR-XANES analysis, which had no effect on mercury isotope ratios (Figure S1). Delta values of MDF and mass independent fractionation (MIF) are expressed as $\delta^{XXX}Hg$ and $\Delta^{XXX}Hg$, respectively, in reference to NIST 3133. Isotopic data on certified reference materials and standards are provided in the SI (Table S1).

Results and Discussion

Mercury Speciation in Tissues

The Hg L_3-edge HR-XANES spectra from the three birds show distinct and consistent shifts among tissues that are diagnostic of differences in mercury speciation (Figure 1). The Clark's grebe tissues exhibit the most dramatic differences with mercury present as 100% MeHg-Cys in the brain (indicated by the sharp near-edge peak at 12,279.8 eV unique to MeHg-Cys)[23,36] and a progressive decrease in the amplitude of the near-edge MeHg-Cys peak in the muscle, kidneys, and liver spectra. As detailed previously,[4] spectral shifts in the Clark's grebe tissues are due to an increasing percentage of mercury as $Hg(Sec)_4$ (0%, 11%, 59%, and 86% in brain, muscle, kidneys, and liver, respectively; Table 1, Table S2). A minor component of Hg-dithiolate complex ($Hg(SR)_2$) is observed in the muscle (23%) and kidneys (12%) (Table 1). In the Forster's tern, mercury is present solely as MeHg-Cys in the brain and muscle (100% MeHg-Cys), and the kidneys and liver exhibit increasing proportions of mercury as $Hg(Sec)_4$ (85% MeHg-Cys + 15% $Hg(Sec)_4$ and 75% MeHg-Cys + 25% $Hg(Sec)_4$, respectively; Table 1). Similarly, the south polar skua shows comparable differences between muscle (100% MeHg-Cys) and liver tissues (83% MeHg-Cys + 17% $Hg(Sec)_4$). There is no spectroscopic evidence for nanoparticulate HgSe, as observed in southern giant petrel by HR-XANES.[22] All tissues were modeled with high precision (Table S2) due to excellent species resolution of HR-XANES (e.g., see reference spectra in Figure 1). Good agreement is observed between %MeHg-Cys measured by HR-XANES and %MeHg measured by chemical measurements (Figure S2), consistent with a previous comparison.[4]

The iHg speciation correlates to the THg concentration between bird tissues. For the Clark's grebe and Forster's tern, THg concentrations of tissues (muscle, kidneys, liver) were normalized to that of the brain, which exhibited 100% MeHg-Cys. A robust positive correlation is observed between $\%Hg(Sec)_4$ and the relative THg concentration of each tissue to the brain (Figure S3). Molar concentrations of Se to Hg as $Hg(Sec)_4$ (Se:$Hg(Sec)_4$ ratio) are >4 in the Forster's tern kidneys and liver and south polar skua liver, consistent with the spectroscopic evidence that tissues contain $Hg(Sec)_4$ (Figure S4). The Clark's grebe kidneys and liver tissues exhibit $1 < Se:Hg(Sec)_4 < 4$, suggesting the co-presence of mononuclear $Hg(Sec)_4$ complexes and disordered $Hg_x(Se,Sec)_y$ clusters.[4]

Mass-Dependent Fractionation via Biotic Demethylation

Mercury isotope ratios showed clear evidence for MDF in tissues that have a mixture of MeHg-Cys and iHg species ($Hg(Sec)_4$, $Hg(SR)_2$) (Figure 2a; Table 1, Tables S3-S4). Tissular differences between δ^{202}THg and δ^{202}MeHg linearly correlated with the %MeHg-Cys (and hence 100-%iHg), as determined by HR-XANES (Figure 2a), suggesting that variation in δ^{202}THg is the result of mixing of two isotope endmembers (δ^{202}MeHg and δ^{202}iHg). For the Clark's grebe and Forster's tern, δ^{202}THg and δ^{202}MeHg were measured on each tissue (Table 1). For the south polar skua, δ^{202}THg was measured on the muscle and liver and both δ^{202}THg and δ^{202}MeHg were measured on the kidneys. The south polar skua kidneys δ^{202}MeHg (1.25 ± 0.02‰) matched the muscle δ^{202}THg (δ^{202}THg = 1.25 ± 0.10‰; 100% MeHg-Cys), and therefore was representative of δ^{202}MeHg in the muscle and liver. Differences between δ^{202}THg and δ^{202}MeHg were greatest in the Clark's grebe tissues (δ^{202}THg - δ^{202}MeHg = -1.90‰, -1.55‰, and -0.91‰

for the liver, kidneys, and muscle, respectively) followed by Foster's tern liver and kidneys tissues (−0.59‰ and −0.28‰, respectively) and the south polar skua liver (−0.45‰). In the Forster's tern, a modest difference was observed between δ^{202}THg and δ^{202}MeHg values of the muscle (0.22‰) despite no evidence of demethylation, and the δ^{202}MeHg of the liver was within 0.08‰ of the δ^{202}THg of the muscle. Although the Clark's grebe muscle and kidneys contained varying proportions of $Hg(SR)_2$ and $Hg(Sec)_4$, δ^{202}Hg values were consistently light compared to δ^{202}MeHg and statistically aligns with the regression line between δ^{202}THg– δ^{202}MeHg versus %MeHg-Cys (Figure 2a, Figure S5) of tissues where $Hg(Sec)_4$ is the dominant iHg species. Therefore, δ^{202}iHg is considered representative of the dominant $Hg(Sec)_4$ species.

Within each bird, variations of Δ^{199}Hg values and $\Delta^{199}Hg/\Delta^{201}$Hg ratios for both the THg and the MeHg fractions were largely within measurement precision regardless of mercury speciation (Figure 2b; Table 1; Figure S6), consistent with previous observations of the absence of MIF during internal partitioning and transformations of Hg within organisms.[6,9,17,18] Uniformity in Δ^{199}Hg and slope of $\Delta^{199}Hg/\Delta^{201}$Hg between the MeHg and iHg species indicates photochemical demethylation occurs within the food web prior to dietary assimilation of MeHg and likely reflect the bird's prey habitat and foraging behavior.[13,14,37,38]

We interpret isotopic differences between MeHg and $Hg(Sec)_4$ to be the result of a kinetic isotope effect during the *in vivo* demethylation of MeHg → $Hg(Sec)_4$. δ^{202}MeHg exhibited little variation within the Clark's grebe (−0.05 ± 0.18‰, average ± standard deviation, *n*=4) and Forster's tern (0.49 ± 0.14‰, *n*=4) regardless of differences in mercury speciation (Table 1, Figure 2b). Therefore, the isotopic fractionation of mercury in the birds behaved as an open system with an infinite reservoir of reactant (i.e., MeHg). Assuming a unidirectional reaction and instantaneous product,[39] the product-reactant isotopic enrichment factor ($\varepsilon_{Hg(Sec)4/MeHg}$) was determined as the y-intercept of the linear regression between δ^{202}THg– δ^{202}MeHg versus %MeHg-Cys ($\varepsilon_{Hg(Sec)4/MeHg}$ = −2.2 ± 0.1‰; slope ± 95% confidence intervals of fit; Figure 2a). The linear regression weighted each data point to measurement uncertainties.[40] MDF of mercury likely occurs during demethylation of MeHg to $Hg(Sec)_4$, likely by SelP. SelP is rich in selenocysteine residues (*n*≥10 for vertebrates)[4,41] that can facilitate MeHg demethylation[42,43] and was associated with $Hg(Sec)_4$ in the Clark's grebe tissues.[4] Notably, the Clark's grebe kidneys and muscle tissues contained $Hg(SR)_2$ along with $Hg(Sec)_4$. Consistent MDF of tissues that contain $Hg(SR)_2$ and $Hg(Sec)_4$ and those with only $Hg(Sec)_4$ support that $Hg(SR)_2$ is also a byproduct of *in vivo* demethylation of MeHg (Figures 2a, S5), though through an unknown pathway.

We report the first isotopic enrichment factor for *in vivo* demethylation of MeHg by selenium in vertebrates. The magnitude of $\varepsilon_{Hg(Sec)4/MeHg}$ in birds (−2.2 ± 0.1‰) is similar to isotopic differences observed in a range of aquatic mammals (detailed below) but markedly greater than the microbial *mer* pathway ($\varepsilon_{p/r}$ = −0.40 ± 0.20‰).[44] In mammal tissues where species-specific isotopic ratios were determined (δ^{202}MeHg and δ^{202}THg),[16,17] differences between δ^{202}MeHg and δ^{202}iHg pools were estimated to range from −2.1 to ~−3‰ (beluga whale and freshwater seal[16] muscle versus liver, and pilot whale brain tissues).[17] In a study where only δ^{202}THg was measured,[18] the maximum difference in δ^{202}THg between muscle (~100% MeHg) and liver (~6% MeHg) in juvenile pilot whales was ~−2.3‰. Consistent MDF by MeHg demethylation across birds and mammals could be explained by a universal

reaction mechanism involving SelP,[4] which is central to selenium homeostasis.[41] A more detailed comparison of $\varepsilon_{Hg(Sec)4/MeHg}$ to isotope measurements of other birds,[6] fish,[15,19,20] or mammals[9,16–18] would require species-specific isotope ratios and HR-XANES speciation, and knowledge of possible isotope effects from poorly understood processes (e.g., biomineralization of nanoparticulate HgSe from $Hg(Sec)_4$).[22,24] The expression of selenoproteins and insertion efficiency of selenocysteine residues during protein translation can vary between organisms, between tissues, and based on selenium availability,[41,45] and may influence the extent of MeHg demethylation across different organisms[6] and associated isotopic fractionation in environments that differ in selenium availability. Future research efforts are needed to evaluate the mechanisms and isotopic fractionation for MeHg demethylation by SelP, other selenoproteins,[46] and low molecular weight selenium-containing molecule[47], and quantify the variation in $\varepsilon_{Hg(Sec)4/MeHg}$ across diverse organisms and environmental settings (e.g., terrestrial versus marine).

Complementary spectroscopic and isotopic findings shed new light on the toxicokinetics of mercury in birds. Regarding MeHg, tissular δ^{202}MeHg values were not influenced by the local kinetic isotopic effect for the MeHg → $Hg(Sec)_4$ reaction (Figure 2b, Table 1) as would be predicted in a closed system. This observation likely reflects the fast internal cycling of MeHg relative to the demethylation reaction, consistent with observations in birds[6] and marine mammals,[16,17] and dilution of residual heavy δ^{202}MeHg with new dietary MeHg. The δ^{202}MeHg values of the Clark's grebe and Forster's tern feathers, which fingerprint blood mercury isotope ratios during feather growth,[48] were within the narrow range of tissular δ^{202}MeHg values (Table 1). Internal exchange of MeHg leading to uniform δ^{202}MeHg in the birds is consistent with the dynamic nature of MeHg levels in birds due to physiological (e.g., molting, age) and environmental factors (e.g., dietary exposure).[10,27,28,49]

Regarding the toxicokinetics of $Hg(Sec)_4$, correlation between tissular concentrations of THg and $\%Hg(Sec)_4$ (Figure S3) indicates that $Hg(Sec)_4$ is depurated considerably slower than MeHg, consistent with observations between fish muscle versus liver.[4] It is unclear if $Hg(Sec)_4$ and $Hg(SR)_2$ in non-hepatic tissues were demethylated locally or are the result of inter-tissular exchange. Inter-tissular exchange of $Hg(Sec)_4$ or $Hg(SR)_2$ cannot be discounted, has been proposed in birds[6,22] and mammals,[16–18] and is represented in toxicokinetic models,[50] but there is a lack of mechanistic studies in nature. More broadly, *in vivo* demethylation of MeHg has been attributed to positive MDF between dietary MeHg and organism MeHg.[9,17,38,51,52] Quantifying the contribution of MeHg → $Hg(Sec)_4$ or $Hg(SR)_2$ on MDF between dietary and organism MeHg cannot be carried out here and necessitates an improved mechanistic understanding of isotopic fractionation from additional processes (e.g., ligand exchange,[53] $Hg(Sec)_4$ → nanoparticulate HgSe biomineralization).[22] Toxicokinetic models for mercury in birds[54] and mammals[50] will benefit from advancements from emerging techniques described here and elsewhere[4,20,22] that provide a foundation to understand the transformations and redistribution of biologically-relevant mercury species (MeHg, $Hg(SR)_2$, $Hg(Sec)_4$, nanoparticulate HgSe).

Implications on Environmental Applications of Stable Mercury Isotope Ratios

This study demonstrates significant MDF of mercury in bird tissues due to the demethylation of MeHg to primarily $Hg(Sec)_4$.[4] δ^{202}MeHg values were relatively unaffected by MeHg demethylation and therefore direct measurement of δ^{202}MeHg on tissues[20] is recommended for use of δ^{202}Hg for contaminant source apportionment[8–11] in higher-trophic level organisms and on liver or kidney tissues that are not predominantly MeHg.[1,6,9,17,18] It is unknown if isotopically light products of *in vivo* demethylation ($Hg(Sec)_4$ and $Hg(SR)_2$) are transferred within foodwebs (e.g., scavenging of high trophic level organisms at the base of foodwebs).[13,20] Where direct isotopic analysis of the MeHg pool is not feasible, mathematical correction of δ^{202}THg using $\varepsilon_{Hg(Sec)4/MeHg}$ may be warranted in determining the isotopic composition of dietary MeHg sources prior to *in vivo* demethylation. When applying the $\varepsilon_{Hg(Sec)4/MeHg}$ (−2.2 ± 0.1‰), spectroscopic characterization of tissues is encouraged under two scenarios. First, in tissues with high %MeHg (e.g., >80%), HR-XANES analysis should be used to accurately quantify %MeHg due to incomplete recovery of MeHg using traditional chemical techniques (Figure S2 in SI, Figure S4 in Manceau et al. 2021,[4] Figure S2 in Bolea-Fernandez et al. 2019).[18] Second, in tissues with low %MeHg (e.g., <30%), HR-XANES analysis is necessary to detect co-occurrence of $Hg(Sec)_4$ and nanoparticulate HgSe.[22] It remains unknown if the biomineralization of nanoparticulate HgSe from $Hg(Sec)_4$ induces positive or negative MDF based on observation in marine bird[6] and mammal tissues with very low %MeHg.[16–18,24]

Supporting Information

Descriptions of measurements; mercury isotope ratios for CRMs, standards, and samples (Table S1, S3, and S4; Figure S1 and S6); HR-XANES spectra fit results (Table S2); comparison of %MeHg by HR-XANES and chemical analysis (Figure S2); correlations between THg concentration and iHg speciation (Figure S3); ratios of Se to Hg (Figure S4); comparison of isotope versus $\%Hg(Sec)_4$ by HR-XANES results (Figure S5) (PDF). HR-XANES spectra (XLXS).

Acknowledgments

We thank Pieter Glatzel, Blanka Detlefs (European Synchrotron Radiation Facility), and Kathy Nagy (University of Illinois at Chicago) for support during data collection on beamline ID26. We thank Mike Tate, Jake Ogorek, John Pierce, and Caitlin Rumrill (U.S. Geological Survey) for assistance with mercury isotope and concentration measurements. We acknowledge Brooke Hill, Jeong-Hoon Kim, and Josh Ackerman for photos of the Forster's tern, south polar skua, and Clark's grebe used in the TOC art. We thank Ryan Lepak (US EPA) and two anonymous reviewers for constructive feedback on the manuscript. Financial support was provided to B.A.P. by the U.S. National Science Foundation under grant EAR-1629698, to B.A.P., S.E.J., A.R.S., D.P.K., C.A.E., and J.T.A. by the U.S. Geological Survey (USGS) Environmental Health Mission Area's Toxic Substances Hydrology and Contaminants Biology Programs, and to A.R.S. by the Water Mission Area. Financial support was provided to A.M. by the French National Research Agency (ANR) under grant ANR-10-EQPX-27-01 (EcoX Equipex), and to E.K. and J.H.K. by the

Ecosystem Structure and Function of Marine Protected Area (MPA) in Antarctica' project (PM20060), funded by the Ministry of Oceans and Fisheries (20170336), Korea. Any use of trade, firm, or product names is for descriptive purposes only and does not imply endorsement by the U.S. Government.

References

(1) Chételat, J.; Ackerman, J. T.; Eagles-Smith, C. A.; Hebert, C. E. Methylmercury exposure in wildlife: A review of the ecological and physiological processes affecting contaminant concentrations and their interpretation. *Sci. Total Environ.* **2020**, *711*, DOI: 10.1016/j.scitotenv.2019.135117.

(2) Harris, H. H.; Pickering, I. J.; George, G. N. The chemical form of mercury in fish. *Science* **2003**, *301*, 1203, DOI: 10.1126/science.1085941.

(3) Bourdineaud, J. P.; Gonzalez-Rey, M.; Rovezzi, M.; Glatzel, P.; Nagy, K. L.; Manceau, A. Divalent mercury in dissolved organic matter Is bioavailable to fish and accumulates as dithiolate and tetrathiolate complexes. *Environ. Sci. Technol.* **2019**, *53*, 4880-4891, DOI: 10.1021/acs.est.8b06579.

(4) Manceau, A.; Bourdineaud, J. P.; Oliveira, R. B.; Sarrazin, S. L. F.; Krabbenhoft, D. P.; Eagles-Smith, C. A.; Ackerman, J. T.; Stewart, A. R.; Ward-Deitrich, C.; del Castillo Busto, M. E.; Goenaga-Infante, H.; Wack, A.; Retegan, M.; Detlefs, B.; Glatzel, P.; Bustamante, P.; Nagy, K. L.; Poulin, B. A. Demethylation of methylmercury in bird, fish, and earthworm. *Environ. Sci. Technol.* **2021**, 55, 1527-1534, DOI: 10.1021/acs.est.0c04948.

(5) Eagles-Smith, C. A.; Ackerman, J. T.; Julie, Y. E. E.; Adelsbach, T. L. Mercury demethylation in waterbird livers: Dose-response thresholds and differences among species. *Environ. Toxicol. Chem.* **2009**, *28*, 568-577, DOI: 10.1897/08-245.1.

(6) Renedo, M.; Pedrero, Z.; Amouroux, D.; Cherel, Y.; Bustamante, P. Mercury Isotopes of Key Tissues Document Mercury Metabolic Processes in Seabirds. *Chemosphere* **2021**, *263*, 127777, DOI: 10.1016/j.chemosphere.2020.127777.

(7) Ackerman, J. T.; Herzog, M. P.; Evers, D. C.; Cristol, D. A.; Kenow, K. P.; Heinz, G. H.; Lavoie, R. A.; Brasso, R. L.; Mallory, M. L.; Provencher, J. F.; Braune, B. M.; Matz, A.; Schmutz, J. A.; Eagles-Smith, C. A.; Savoy, L. J.; Meyer, M. W.; Hartman, C. A. Synthesis of maternal transfer of mercury in birds: Implications for altered toxicity risk. *Environ. Sci. Technol.* **2020**, *54*, 2878–2891, DOI: 10.1021/acs.est.9b06119.

(8) Li, M.; Schartup, A. T.; Valberg, A. P.; Ewald, J. D.; Krabbenhoft, D. P.; Yin, R.; Balcom, P. H.; Sunderland, E. M. Environmental origins of methylmercury accumulated in subarctic estuarine fish indicated by mercury stable isotopes. *Environ. Sci. Technol.* **2016**, *50*, 11559-11568, DOI: 10.1021/acs.est.6b03206.

(9) Masbou, J.; Sonke, J. E.; Amouroux, D.; Guillou, G.; Becker, P. R.; Point, D. Hg-stable isotope variations in marine top predators of the western Arctic Ocean. *ACS Earth Sp. Chem.* **2018**, *2*,

479-490, DOI: 10.1021/acsearthspacechem.8b00017.

(10) Renedo, M.; Amouroux, D.; Pedrero, Z.; Bustamante, P.; Cherel, Y. Identification of sources and bioaccumulation pathways of MeHg in subantarctic penguins: A stable isotopic investigation. *Sci. Rep.* **2018**, *8*, DOI: 10.1038/s41598-018-27079-9.

(11) Lepak, R. F.; Janssen, S. E.; Yin, R.; Krabbenhoft, D. P.; Ogorek, J. M.; DeWild, J. F.; Tate, M. T.; Holsen, T. M.; Hurley, J. P. Factors affecting mercury stable isotopic distribution in piscivorous fish of the Laurentian Great Lakes. *Environ. Sci. Technol.* **2018**, *52*, 2768–2776. DOI: 10.1021/acs.est.7b06120.

(12) Lepak, R. F.; Hoffman, J. C.; Janssen, S. E.; Krabbenhoft, D. P.; Ogorek, J. M.; DeWild, J. F.; Tate, M. T.; Babiarz, C. L.; Yin, R.; Murphy, E. W.; Engstrom, D. R.; Hurley, J. P. Mercury source changes and food web shifts alter contamination signatures of predatory fish from Lake Michigan. *Proc. Natl. Acad. Sci. U. S. A.* **2019**, *116*, 23600-23608, DOI: 10.1073/pnas.1907484116.

(13) Blum, J. D.; Drazen, J. C.; Johnson, M. W.; Popp, B. N.; Motta, L. C.; Jamieson, A. J. Mercury isotopes identify near-surface marine mercury in deep-sea trench biota. *Proc. Natl. Acad. Sci.* **2020**, *117*, 29292-29298, DOI: 10.1073/pnas.2012773117.

(14) Blum, J. D.; Sherman, L. S.; Johnson, M. W. Mercury isotopes in earth and environmental sciences. *Annu. Rev. Earth Planet. Sci.* **2014**, *42*, 249–269, DOI: 10.1146/annurev-earth-050212-124107.

(15) Rua-Ibarz, A.; Bolea-Fernandez, E.; Maage, A.; Frantzen, S.; Sanden, M.; Vanhaecke, F. Tracing mercury pollution along the Norwegian coast via elemental, speciation, and isotopic analysis of liver and muscle tissue of deep-water marine fish (*Brosme Brosme*). *Environ. Sci. Technol.* **2019**, *53*, 1776-1785, DOI: 10.1021/acs.est.8b04706.

(16) Perrot, V.; Masbou, J.; Pastukhov, M. V.; Epov, V. N.; Point, D.; Bérail, S.; Becker, P. R.; Sonke, J. E.; Amouroux, D. Natural Hg isotopic composition of different Hg compounds in mammal tissues as a proxy for in vivo breakdown of toxic methylmercury. *Metallomics* **2016**, *8*, 170, DOI: 10.1039/c5mt00286a.

(17) Li, M.; Juang, C. A.; Ewald, J. D.; Yin, R.; Mikkelsen, B.; Krabbenhoft, D. P.; Balcom, P. H.; Dassuncao, C.; Sunderland, E. M. Selenium and stable mercury isotopes provide new insights into mercury toxicokinetics in pilot whales. *Sci. Total Environ.* **2020**, *710*, 136325, DOI: 10.1016/j.scitotenv.2019.136325.

(18) Bolea-Fernandez, E.; Rua-Ibarz, A.; Krupp, E. M.; Feldmann, J.; Vanhaecke, F. High-precision isotopic analysis sheds new light on mercury metabolism in long-finned pilot whales (*Globicephala Melas*). *Sci. Rep.* **2019**, *9*, 7262, DOI: 10.1038/s41598-019-43825-z.

(19) Masbou, J.; Point, D.; Sonke, J. E. Application of a selective extraction method for methylmercury compound specific stable isotope analysis (MeHg-CSIA) in biological materials. *J. Anal. At. Spectrom.* **2013**, *28*, 1620-1628, DOI: 10.1039/c3ja50185j.

(20) Rosera, T. J.; Janssen, S. E.; Tate, M. T.; Lepak, R. F.; Ogorek, J. M.; DeWild, J. F.; Babiarz, C. L.; Krabbenhoft, D. P.; Hurley, J. P. Isolation of methylmercury using distillation and anion-exchange chromatography for isotopic analyses in natural matrices. *Anal. Bioanal. Chem.* **2020**, *412*, 681–690, DOI: 10.1007/s00216-019-02277-0.

(21) Manceau, A.; Bustamante, P.; Haouz, A.; Bourdineaud, J. P.; Gonzalez-Rey, M.; Lemouchi, C.; Gautier-Luneau, I.; Geertsen, V.; Barruet, E.; Rovezzi, M.; Glatzel, P.; Pin, S. Mercury(II) binding to metallothionein in *Mytilus Edulis* revealed by high energy-resolution XANES spectroscopy. *Chem. Eur. J.* **2019**, *25*, 997, DOI: 10.1002/chem.201804209.

(22) Manceau, A.; Gaillot, A. C.; Glatzel, P.; Cherel, Y.;Bustamante, P. *In Vivo* formation of HgSe nanoparticles and Hg-tetraselenolate complex from methylmercury in seabird – Implications for the Hg-Se antagonism. *Environ. Sci. Technol.* **2021**, 55, 1515-1526, DOI: 10.1021/acs.est.0c06269.

(23) Manceau, A.; Enescu, M.; Simionovici, A.; Lanson, M.; Gonzalez-Rey, M.; Rovezzi, M.; Tucoulou, R.; Glatzel, P.; Nagy, K. L.; Bourdineaud, J. P. Chemical forms of mercury in human hair reveal sources of exposure. *Environ. Sci. Technol.* **2016**, *50*, 10721-10729, DOI: 10.1021/acs.est.6b03468.

(24) Gajdosechova, Z.; Lawan, M. M.; Urgast, D. S.; Raab, A.; Scheckel, K. G.; Lombi, E.; Kopittke, P. M.; Loeschner, K.; Larsen, E. H.; Woods, G.; Brownlow, A.; Read, F. L.; Feldmann, J.; Krupp, E. M. In vivo formation of natural HgSe nanoparticles in the liver and brain of pilot whales. *Sci. Rep.* **2016**, *6*, 34361, DOI: 10.1038/srep34361.

(25) Nakazawa, E.; Ikemoto, T.; Hokura, A.; Terada, Y.; Kunito, T.; Tanabe, S.; Nakai, I. The presence of mercury selenide in various tissues of the striped dolphin: Evidence from μ-XRF-XRD and XAFS analyses. *Metallomics* **2011**, *3*, 719–725, DOI: 10.1039/C0MT00106F.

(26) Arai, T.; Ikemoto, T.; Hokura, A.; Terada, Y.; Kunito, T.; Tanabe, S.; Nakai, I. Chemical forms of mercury and cadmium accumulated in marine mammals and seabirds as determined by XAFS analysis. *Environ. Sci. Technol.* **2004**, *38*, 6468-6474, DOI: 10.1021/es040367u.

(27) Hartman, C. A.; Ackerman, J. T.; Herzog, M. P.; Eagles-Smith, C. A. Season, molt, and body size influence mercury concentrations in grebes. *Environ. Pollut.* **2017**, *229*, 29-39, DOI: 10.1016/j.envpol.2017.05.058.

(28) Ackerman, J. T.; Eagles-Smith, C. A.; Takekawa, J. Y.; Bluso, J. D.; Adelsbach, T. L. Mercury concentrations in blood and feathers of prebreeding Forster's terns in relation to space use of San Francisco Bay, California, USA, Habitats. *Environ. Toxicol. Chem.* **2008**, *27*, 897-908, DOI: 10.1897/07-230.1.

(29) Poulin, B. A.; Manceau, A.; Krabbenhoft, D. P.; Stewart, A. R.; Ward-Deitrich, C.; del Castillo Busto, M. E.; Goenaga-Infante, H.; Bustamante, P. Mercury and selenium chemical characteristics and speciation data of bird, fish, and earthworm tissues. *U.S. Geological Survey Data Release* **2020**, DOI: 10.5066/P96NP376.

(30) Rovezzi, M.; Lapras, C.; Manceau, A.; Glatzel, P.; Verbeni, R. High energy-resolution X-ray spectroscopy at ultra-high dilution with spherically bent crystal analyzers of 0.5 m radius. *Rev. Sci. Instrum.* **2017**, *88*, 013108, DOI: 10.1063/1.4974100.

(31) Mah, V.; Jalilehvand, F. Glutathione complex formation with mercury(II) in aqueous solution at physiological pH. *Chem. Res. Toxicol.* **2010**, *23*, 1815-1823, DOI: 10.1021/tx100260e.

(32) Manceau, A.; Wang, J.; Rovezzi, M.; Glatzel, P.; Feng, X. Biogenesis of mercury–sulfur nanoparticles in plant leaves from atmospheric gaseous mercury. *Environ. Sci. Technol.* **2018**, *52*, 3935–3948, DOI: 10.1021/acs.est.7b05452.

(33) Kleckner, A. E.; Kakouros, E.; Robin Stewart, A. A practical method for the determination of total selenium in environmental samples using isotope dilution-hydride generation-inductively coupled plasma-mass spectrometry. *Limnol. Oceanogr. Methods* **2017**, *15*, 363–371, DOI: 10.1002/lom3.10164.

(34) Janssen, S. E.; Lepak, R. F.; Tate, M. T.; Ogorek, J. M.; DeWild, J. F.; Babiarz, C. L.; Hurley, J. P.; Krabbenhoft, D. P. Rapid pre-concentration of mercury in solids and water for isotopic analysis. *Anal. Chim. Acta* **2019**, *1054*, 95-103, DOI: 10.1016/j.aca.2018.12.026.

(35) Yin, R.; Krabbenhoft, D. P.; Bergquist, B. A.; Zheng, W.; Lepak, R. F.; Hurley, J. P. Effects of mercury and thallium concentrations on high precision determination of mercury isotopic composition by Neptune Plus multiple collector inductively coupled plasma mass spectrometry. *J. Anal. At. Spectrom.* **2016**, *31, 2060-2068*, DOI: 10.1039/c6ja00107f.

(36) Thomas, S. A.; Mishra, B.; Myneni, S. C. B. Cellular mercury coordination environment, and not cell surface ligands, influence bacterial methylmercury production. *Environ. Sci. Technol.* **2020**, *54*, 3960-3968, DOI: 10.1021/acs.est.9b05915.

(37) Bergquist, B. A.; Blum, J. D. Mass-dependent and -independent fractionation of Hg isotopes by photoreduction in aquatic systems. *Science* **2007**, *318*, 417-420, DOI: 10.1126/science.1148050.

(38) Perrot, V.; Pastukhov, M. V.; Epov, V. N.; Husted, S.; Donard, O. F. X.; Amouroux, D. Higher mass-independent isotope fractionation of methylmercury in the pelagic food web of Lake Baikal (Russia). *Environ. Sci. Technol.* **2012**, *46*, 5902-5911, DOI: 10.1021/es204572g.

(39) Mariotti, A.; Germon, J. C.; Hubert, P.; Kaiser, P.; Letolle, R.; Tardieux, A.; Tardieux, P. Experimental determination of nitrogen kinetic isotope fractionation: Some principles; illustration for the denitrification and nitrification processes. *Plant Soil* **1981**, *62*, 413-430, DOI: 10.1007/BF02374138.

(40) York, D. Least-squares fitting of a straight line. *Can. J. Phys.* **1966**, *44*, 1079–1086, DOI: 10.1139/p66-090.

(41) Burk, R. F.; Hill, K. E. Selenoprotein P-expression, functions, and roles in mammals. *Biochim. Biophys. Acta* **2009**, 1790, 1441-1447, DOI: 10.1016/j.bbagen.2009.03.026.

(42) Khan, M. A. K.; Wang, F. Chemical demethylation of methylmercury by selenoamino acids. *Chem. Res. Toxicol.* **2010**, *23*, 1202-1206, DOI: 10.1021/tx100080s.

(43) Asaduzzaman, A. M.; Schreckenbach, G. Degradation mechanism of methyl mercury selenoamino acid complexes: A computational study. *Inorg. Chem.* **2011**, *50*, 2366-2372, DOI: 10.1021/ic1021406.

(44) Kritee, K.; Barkay, T.; Blum, J. D. Mass dependent stable isotope fractionation of mercury during *mer* mediated microbial degradation of monomethylmercury. *Geochim. Cosmochim. Acta* **2009**, *73*, 1285-1296, DOI: 10.1016/j.gca.2008.11.038.

(45) Penglase, S.; Hamre, K.; Ellingsen, S. The selenium content of SEPP1 versus selenium requirements in vertebrates. *PeerJ* **2015**, 3, e1244, DOI: 10.7717/peerj.1244.

(46) Pickering, I. J.; Cheng, Q.; Rengifo, E. M.; Nehzati, S.; Dolgova, N. V.; Kroll, T.; Sokaras, D.; George, G. N.; Arnér, E. S. J. Direct observation of methylmercury and auranofin binding to selenocysteine in thioredoxin reductase. *Inorg. Chem.* **2020**, *59*, 2711-2718, DOI: 10.1021/acs.inorgchem.9b03072.

(47) Yamashita, Y.; Yamashita, M. Identification of a novel selenium-containing compound, selenoneine, as the predominant chemical form of organic selenium in the blood of bluefin tuna. *J. Biol. Chem.* **2010**, *285*, 18134-18138, DOI: 10.1074/jbc.C110.106377.

(48) Renedo, M.; Amouroux, D.; Duval, B.; Carravieri, A.; Tessier, E.; Barre, J.; Bérail, S.; Pedrero, Z.; Cherel, Y.; Bustamante, P. Seabird tissues as efficient biomonitoring tools for Hg isotopic investigations: Implications of using blood and feathers from chicks and adults. *Environ. Sci. Technol.* **2018**, *52*, 4227-4234, DOI: 10.1021/acs.est.8b00422.

(49) Seewagen, C. L.; Cristol, D. A.; Gerson, A. R. Mobilization of mercury from lean tissues during simulated migratory fasting in a model songbird. *Sci. Rep.* **2016**, *6*, 25762, DOI: 10.1038/srep25762.

(50) Ewald, J. D.; Kirk, J. L.; Li, M.; Sunderland, E. M. Organ-specific differences in mercury speciation and accumulation across ringed seal (*Phoca hispida*) life stages. *Sci. Total Environ.* **2019**, *650*, 2013-2020, DOI: 10.1016/j.scitotenv.2018.09.299.

(51) Sherman, L. S.; Blum, J. D.; Franzblau, A.; Basu, N. New insight into biomarkers of human mercury exposure using naturally occurring mercury stable isotopes. *Environ. Sci. Technol.* **2013**, *47*, 3403-3409, DOI: 10.1021/es305250z.

(52) Laffont, L.; Sonke, J. E.; Maurice, L.; Monrroy, S. L.; Chincheros, J.; Amouroux, D.; Behra, P. Hg speciation and stable isotope signatures in human hair as a tracer for dietary and occupational exposure to mercury. *Environ. Sci. Technol.* **2011**, *45*, 9910-9916, DOI: 10.1021/es202353m.

(53) Wiederhold, J. G.; Cramer, C. J.; Daniel, K.; Infante, I.; Bourdon, B.; Kretzschmar, R. Equilibrium mercury isotope fractionation between dissolved Hg(II) species and thiol-bound Hg. *Environ. Sci. Technol.* **2010**, *44*, 4191–4197, DOI: 10.1021/es100205t.

(54) Bearhop, S.; Ruxton, G. D.; Furness, R. W. Dynamics of mercury in blood and feathers of great skuas. *Environ. Toxicol. Chem.* **2000**, *19*, 1638-1643, DOI: 10.1002/etc.5620190622.

Figures and Tables

Table 1. Chemical, spectroscopic, and isotopic data of bird tissue and feather samples.

	--------- Chemical Meas. ---------[a]			---------- HR-XANES fit results ----------[b]			---------- Species-specific isotope ratios ----------			
Tissue	**THg (mg/kg)**	**MeHg (mg/kg)**	**Se (mg/kg)**	**%MeHg-Cys**	**%Hg(Sec)$_4$**	**%Hg(SR)$_2$**	**δ^{202}THg (±1SD)**	**Δ^{199}THg (±1SD)**	**δ^{202}MeHg (±1SD)**	**Δ^{199}MeHg (±1SD)**
Clark's grebe (*A. clarkii*)										
Brain	3.18	2.98	1.55	100	0	0	0.07	1.51	0.06	1.49
							(0.03)	(0.03)	(0.04)	(0.02)
Muscle	7.10	3.71	2.31	66	11	23	-1.13	1.46	-0.22	1.43
							(0.04)	(0.04)	(0.03)	(0.02)
Kidneys	21.6	6.38	10.6	28	59	12	-1.41	1.42	0.14	1.45
							(0.03)	(0.04)	(0.02)	(0.03)
Liver	43.1	7.86	19.3	14	86	0	-2.07	1.49	-0.17	1.42
							(0.04)	(0.04)	(0.02)	(0.02)
Breast Feather	41.4	32.7	1.04	100	0	0	0.15 (0.03)	1.77 (0.02)	0.13 (0.05)	2.04 (0.03)
Forster's tern (*S. forsteri*)										
Brain	5.28	4.48	3.31	100	0	0	0.51	0.68	0.57	0.81
							(0.02)	(0.02)	(0.01)	(0.02)
Muscle	6.39	5.65	3.33	100	0	0	0.53	0.72	0.31	0.79
							(0.03)	(0.03)	(0.02)	(0.02)
Kidneys	12.6	9.21	9.64	85	15	0	0.34	0.70	0.62	0.66
							(0.02)	(0.03)	(0.03)	(0.02)
Liver	13.8	9.22	6.21	75	25	0	-0.14	0.67	0.45	0.71
							(0.02)	(0.03)	(0.04)	(0.08)
Breast Feather	28.6	18.2	1.41	100	0	0	0.70 (0.03)	1.65 (0.04)	0.72 (0.02)	1.81 (0.04)
south polar skua (*S. maccormicki*)										
Muscle	1.75	1.39	19.4	100	0	0	1.25	1.99	--	--
							(0.05)	(0.03)		
Kidneys	8.61	4.56	--	--	--	--	0.17	2.00	1.25	1.92
							(0.03)	(0.05)	(0.01)	(0.01)
Liver	8.19	6.39	29.7	83	17	0	0.80	2.02	--	--
							(0.01)	(0.04)		

[a] reported on a dry weight basis.

[b] precision of fit results are 5% for the Clark's grebe tissues[4] and 10% for Forster's tern and south polar skua tissues (see SI Table S2).

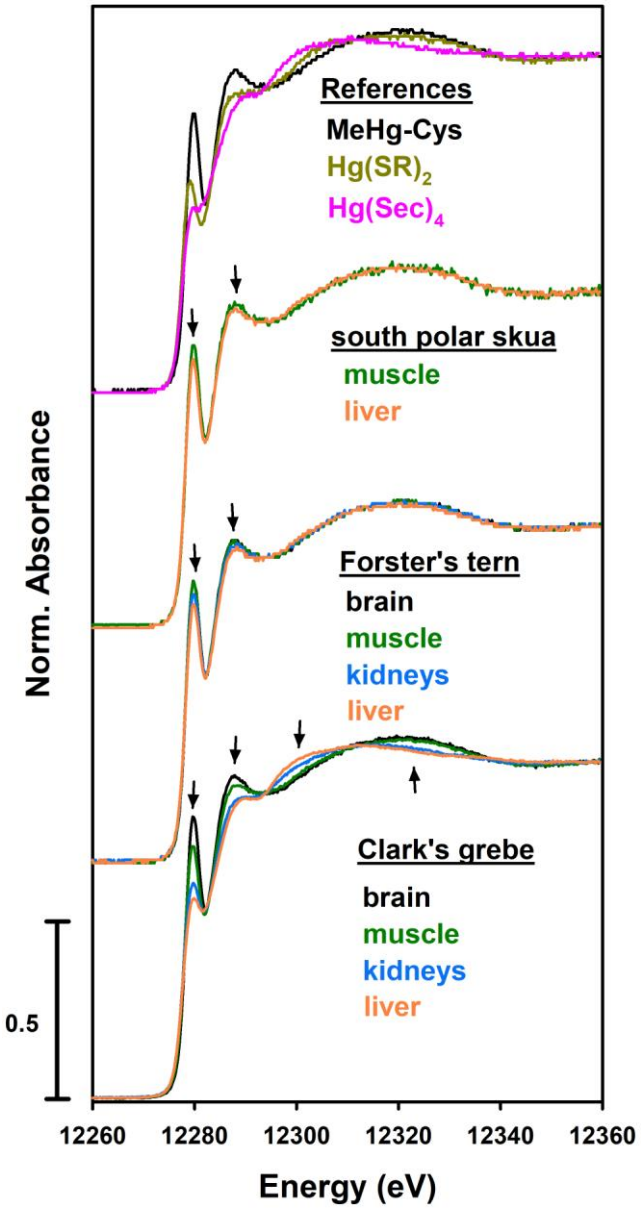

Figure 1. Hg L_3-edge HR-XANES spectra of tissues from a Clark's grebe, Forster's tern, and south polar skua (brain, black; muscle, green; kidneys, blue; liver, orange). Black arrows identify regions of the spectra that differ with shifts in mercury speciation primarily in the proportion of MeHg-Cys and $Hg(Sec)_4$. References spectra are shown for the three species observed in the tissues (MeHg-Cys; $Hg(SR)_2$; $Hg(Sec)_4$).

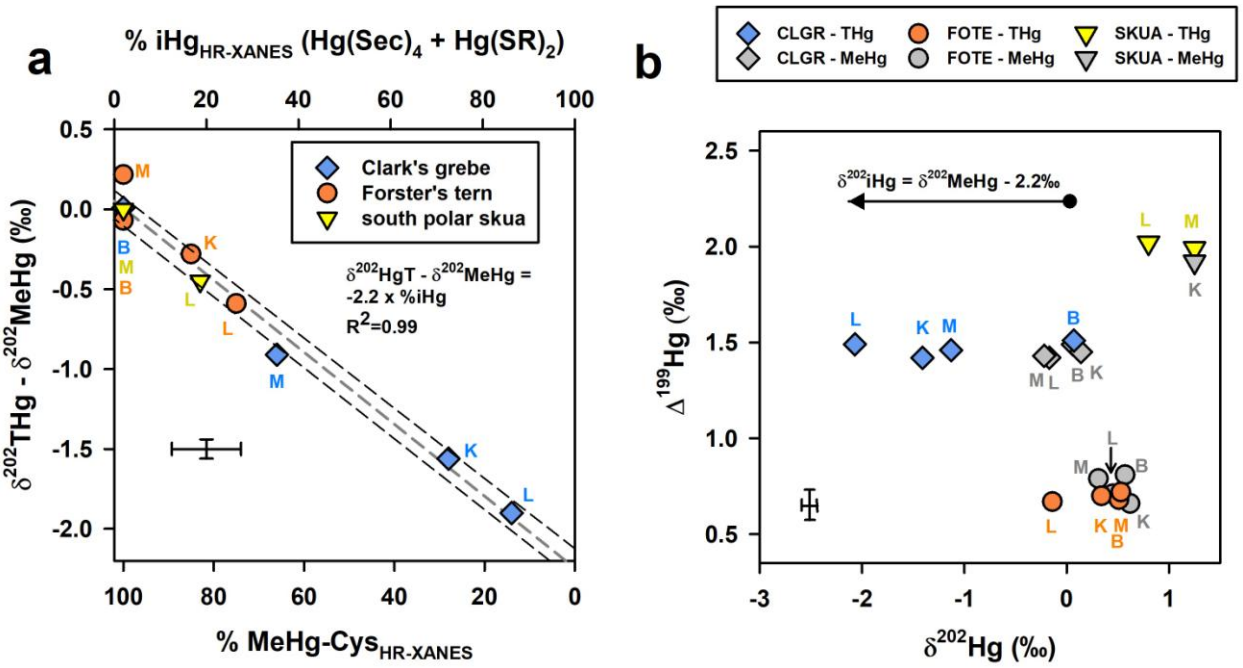

Figure 2. (**a**) Relationship between the difference in δ^{202}Hg values of total mercury minus methylmercury (δ^{202}THg – δ^{202}MeHg; Table 1) and the speciation of mercury as determined by HR-XANES of bird tissues; data are weighted to uncertainties of both X and Y variables. (**b**) Biplot of Δ^{199}Hg versus δ^{202}Hg of total mercury (THg; color-filled symbols) and methylmercury (MeHg; gray-filled symbols) for bird tissues. Single letters abbreviations identify the tissue type (B, brain; K, kidneys; L, liver; M, muscle). Generic error bars present uncertainties of isotope measurements (2SD) and HR-XANES fits (Table S2). In plot **a** the dashed gray and black lines present the fit of data and 95% confidence interval of the fit, respectively.

Supporting Information

to

Isotope Fractionation from *In Vivo* Methylmercury Detoxification in Waterbirds

Brett A. Poulin[a,b*], Sarah E. Janssen[c], Tylor J. Rosera[c,d], David P. Krabbenhoft[c], Collin A. Eagles-Smith[e], Joshua T. Ackerman[f], A. Robin Stewart[g], Eunhee Kim[h], Zofia Baumann[i], Jeong-Hoon Kim[j], and Alain Manceau[j*]

[a]Department of Environmental Toxicology, University of California Davis, Davis, CA 95616, USA (current address)
[b]U.S. Geological Survey, Water Mission Area, Boulder, Colorado 80303, United States
[c]U.S. Geological Survey, Upper Midwest Water Science Center, Middleton, Wisconsin 53562, United States
[d]Environmental Chemistry and Technology Program, University of Wisconsin-Madison, Madison, WI 53706, USA
[e]U.S. Geological Survey, Forest and Rangeland Ecosystem Science Center, Corvallis, Oregon, 97331, United States
[f]U.S. Geological Survey, Western Ecological Research Center, Dixon Field Station, Dixon, California, 95620, United States
[g]U.S. Geological Survey, Water Mission Area, Menlo Park, California, USA
[h]Citizens' Institute for Environmental Studies (CIES), Seoul, Korea
[i]Department of Marine Sciences, University of Connecticut, Groton, CT 06340, USA
[j]Division of Life Sciences, Korea Polar Research Institute, Incheon, Korea
[k]University Grenoble Alpes, ISTerre, CNRS, CS 40700, 38058 Grenoble, France

* Corresponding authors. Tel: +1 530 754 2454. *Email address:* bapoulin@ucdavis.edu (B.A. Poulin), alain.manceau@univ-grenoble-alpes.fr (A. Manceau)

Supporting information includes 6 Figures, 4 Tables, and 12 pages.

Contents

Chemical Measurements S18
Mercury Isotope Measurements S19
HR-XANES Spectra Acquisition and Fitting S20
Figure and Tables S21

References S29

Chemical Measurements

Concentrations of total mercury (THg), methylmercury (MeHg), and total selenium (T-Se) were determined identical to that described in Manceau et al. 2021.[1] Total Hg and MeHg were quantified at the U.S. Geological Survey Mercury Research Laboratory (Middleton, Wisconsin) on tissues on a dry weight basis. Tissues were processed using a nitric acid (4.5 M) extraction and heated at 55 °C for 8 hours. First, MeHg was quantified on an aliquot of extracts by aqueous phase ethylation, trapping on Tenax® (Buchem B.V.), isothermal gas chromatography separation, and cold vapor atomic fluorescence spectroscopy (CVAFS) detection using a Brooks Rand MERX-M following U.S. Environmental Protection Agency Method 1630. Second, tissue extracts were further oxidized with sodium persulfate (2% of final volume) overnight and brominated to a final volume of 10% bromine monochloride (BrCl). Oxidized extracts were measured for total Hg via stannous chloride reduction and gold amalgamation coupled to CVAFS detection using a Brooks Rand MERX-T following U.S. Environmental Protection Agency Method 1631. The standard deviation between digestion triplicates for MeHg was ≤ 5.2% (n = 3), the recovery of MeHg from IAEA-436 reference (n = 9; certified at 0.200 ± 0.010 mg MeHg kg^{-1} dry weight) averaged 92%, and the recovery of MeHg from quality control spikes averaged 99% (n = 17). The standard deviation between digestion triplicates for total Hg was ≤ 8.6% (n = 4), the recovery of Hg from IAEA-436 reference (n = 9; certified at 0.220 ± 0.010 mg Hg kg^{-1} dry weight) averaged 98%, and the recovery of Hg from quality control spikes averaged 99% (n = 14).

Selenium concentrations were determined on all samples by isotope dilution-hydride generation-inductively coupled plasma-mass spectrometry (ID-HG-ICP-MS)[2] at the U.S. Geological Survey (Menlo Park, California). Quality assurance and quality control were assessed by procedural blanks (run in triplicate), duplicate digestions (n = 10), and certified reference materials that spanned a range of sample matrices (run in triplicate with each run). Se recoveries for certified reference materials averaged 106% (n = 6) for National Institute of Science and Technology (NIST2976) mussel tissue, 102% (n = 6) for National Research Council Canada (NRCC) dogfish muscle (DORM2), 96% (n = 6) for NRCC dogfish liver (DOLT3), 93% (n = 3) for NRCC lobster hepatopancreas (TORT3), and 115% (n = 3) for NRCC marine sediment (MESS-3). Procedural blanks were always less than 10% of sample concentrations and averaged 0.010 mg kg^{-1} dry weight (based on an average sample mass of 10 mg) and precision for samples run in duplicate averaged 3.0% (calculated as the absolute deviation divided by the mean, as a percent).

Mercury Isotope Measurements

Mercury isotope measurements were made on tissues for the total Hg and the MeHg fraction. When measurements for MeHg and total Hg isotopes were performed on the same tissue, two separate aliquots of dried material were processed. For total Hg isotope analysis, tissues were subject to a step-wise digestion. First, tissues were prepared via heated acid digestions (concentrated HNO_3) for 8 hours. Next, sample digests were further treated with bromine monochloride (BrCl) to 10% of the total volume and heated for an additional 2 hours to ensure the oxidation of any organic Hg species. Samples were diluted to 5% H^+ content prior to isotope analysis. Concentration recoveries for digestions of certified refence material (IAEA-407, fish homogenate) averaged 93% (*n* = 3).

MeHg isotope measurements were performed on all tissues using a previously established distillation and anion-exchange resin method.[3] Briefly, samples were distilled to removed matrix interferences and distillates were preserved to a final acid concentration of 1 mM hydrochloric acid (HCl). After acidification, samples were passed through a pre-treated AG1-X4 resin column.[3] MeHg is neutrally charged at 1 mM HCl conditions and therefore does not sorb to the AG1-X4 resin, whereas negatively charged inorganic Hg species were sorbed to the AG1-X4 resin. The eluent from the column was collected, oxidized, and confirmed for concentration recovery of MeHg by the measurement of HgT. Determination of Hg recovery was based on the calculated amount of MeHg originally distilled. If required, large volumes of eluent were further pre-concentrated using a sequence of stannous chloride reduction and purge to gold trap for amalgamation, subsequent semi-rapid thermal release (35-minutes), and collection into an oxidant trap.[4] Concentration recoveries of processed samples were >90%. Certified reference material DORM-2 was also processed with samples in duplicate and had recoveries of 101 and 94% (*n* = 2). Replicates for MeHg isotope pre-concentration exhibited acceptable concentration recovery of MeHg on the Clark's grebe kidneys (average 7% difference, *n* =2) and Forster's tern liver (average 1% difference, *n* =3) tissues.

Isotope measurements of the total Hg and MeHg pools were made using a multicollector inductively coupled plasma mass spectrometer (MC-ICP-MS, Neptune Plus, Thermo Scientific). Analysis was conducted using standard-sample bracketing with NIST 3133. Mercury isotope ratios are expressed in delta notation and reported as per mille (‰) in reference to NIST 3133. All samples were matrix and concentration matched (within 10%) of prepared NIST standards. Delta values of MDF are denoted as $\delta^{XXX}Hg$:

$$\delta^{XXX}Hg\ (‰) = [\ (^{XXX}Hg/^{198}Hg_{sample}) / (^{XXX}Hg/^{198}Hg_{NIST\ 3133}) -1] \times 1000 \quad (S1)$$

where XXX represents the specified Hg isotope and $^{198}Hg_{NIST\ 3133}$ is the isotopic signature of NIST 3133. Mass independent fraction (MIF) of both even and odd isotopes was calculated as:

$$\Delta^{XXX}Hg\ (‰) \approx \delta^{XXX}Hg - (\delta^{202}Hg * \beta) \qquad (S2)$$

where β represents the mass scaling factor. Standards, samples, and reference materials were introduced to the MC-ICP-MS using stannous chloride reduction in a custom gas liquid separator[5] at a flow rate of 0.85 mL min^{-1}. A thallium standard (Tl, NIST 997, 200 mM) was simultaneously introduced to the gas-liquid separator for mass bias correction using a desolvating nebulizer (Apex-Q, ESI). The MC-ICP-MS was tuned for optimal voltage and signal intensity for ^{202}Hg and ^{205}Tl prior to analysis. A secondary standard (NIST RM 8610, UM Almadén) was run every five samples to ensure external accuracy and precision of measurements ($\delta^{202}Hg$ = -0.55 ± 0.06‰, $\Delta^{199}Hg$ = -0.02 ± 0.06‰, $\Delta^{200}Hg$ = 0.01 ± 0.04‰, 2SD, *n* = 31). Certified reference materials for HgT and species-specific measurements were comparable to literature values (Table S1).[3] Replicate MeHg extracts for isotope measurements shows good reproducibility for both the Clark's grebe kidneys tissue ($\delta^{202}Hg$ = 0.14 ± 0.04‰, $\Delta^{199}Hg$ = 1.45 ± 0.06‰, $\Delta^{200}Hg$ = 0.04 ± 0.02, 2SD, *n* = 2) and Forster's tern liver tissue ($\delta^{202}Hg$ = -0.45 ± 0.08‰, $\Delta^{199}Hg$ = 0.71 ± 0.16‰, $\Delta^{200}Hg$ = 0.03 ± 0.03, 2SD, *n* = 3).

HR-XANES Spectra Acquisition and Fitting

All freeze-dried samples were pressed into 5.0 mm diameter and 2.5 mm thick pellets, mounted in a polyether ether ketone (PEEK) sample holder sealed with Kapton tape, and maintained in a desiccator until their transfer into the liquid helium cryostat of the beamline. Mercury L_3-edge HR-XANES and HR-EXAFS spectra were measured with high-reflectivity analyzer crystals[6] on beamline ID26 at the European Synchrotron Radiation Facility (ESRF). The storage ring was operated in the 7/8 + 1 filling mode, with 200 mA current. Rejection of higher harmonics and reduction of heat load were achieved with a white beam Pd-coated, flat mirror working under total reflection at 2.5 mrad deflecting angle. The energy of the incoming beam was selected by the 111 reflection of a Si double crystal monochromator, and the beam was focused horizontally by a second Pd-coated mirror and vertically by a third Pd-coated mirror. The flux on the sample was approximately 10^{13} photon/s in a beam footprint of ~700 (H) x 80 (V) μm^2 full width at half maximum (FWHM). The Hg $L_{\alpha 1}$ ($3d_{5/2} \rightarrow 2p_{3/2}$) fluorescence line was selected using the 555 reflection of five spherically bent (radius = 0.5 m)[6] Si analyzer crystals (diameter = 100 mm) aligned at 81.8° Bragg angle in a vertical Rowland geometry. The diffracted intensity was measured with a Si drift diode detector (SDD) in single photon counting mode. The effective energy resolution, obtained by convoluting the total instrument energy bandwidth (spreads of the incident and emitted rays) and the $3d_{5/2}$ core-hole width from the $L_{\alpha 1}$ line was about 3.0 eV, compared to an intrinsic line broadening of about 6.1 eV in conventional fluorescence yield measurement with a solid-state detector (conventional XANES).

The incident energy was scanned from 12,260 eV to 12,360 eV in 0.2 eV steps, and the spectra were normalized to unity at E = 12,360 eV. The stability in energy of the incident beam was monitored by measuring frequently a fresh MeHg-cysteine (MeHg-Cys) reference. The photon energy is referenced to the maximum of the near-edge peak of MeHg-Cys at 12,279.8 eV. The precision of the calibrated spectra

is 0.1 eV. Spectra were collected at a temperature of 10-15 K and a scan time of 15 seconds to reduce exposure, and repeated at different pristine positions on the sample to increase the signal-to-noise ratio and eliminate the possibility for radiation damage of samples.[1]

The proportions of the Hg species in tissues were evaluated using least-squares fitting (LSF) of the data with linear combinations of a diverse set of reference spectra of known structure.[1,7,8] The reference spectrum of MeHg-Cys was represented in spectral fits using the spectrum of the Clark's grebe breast feather. The spectrum of mercury tetraselenolate complex ($Hg(Sec)_4$) was determined by iterative transformation factor analysis.[1] The spectrum of the $Hg(L\text{-glutathione})_2$ complex ($Hg(GSH)_2$) at pH 7.4[9,10] was used as a proxy for mercury dithiolate complex ($Hg(SR)_2$) complex in biota.[11] The precision of estimation of a fit component was estimated to be equal to the variation of its value when the fit residual (NSS) was increased by 20%. NSS is the normalized sum-squared difference between two spectra expressed as:

$$\frac{\sum(y_{exp}-y_{fit})^2}{\sum y_{exp}^2} \qquad \text{(S3)}$$

where y_{exp} and y_{fit} are experimental and fit values, respectively.

Figure and Tables

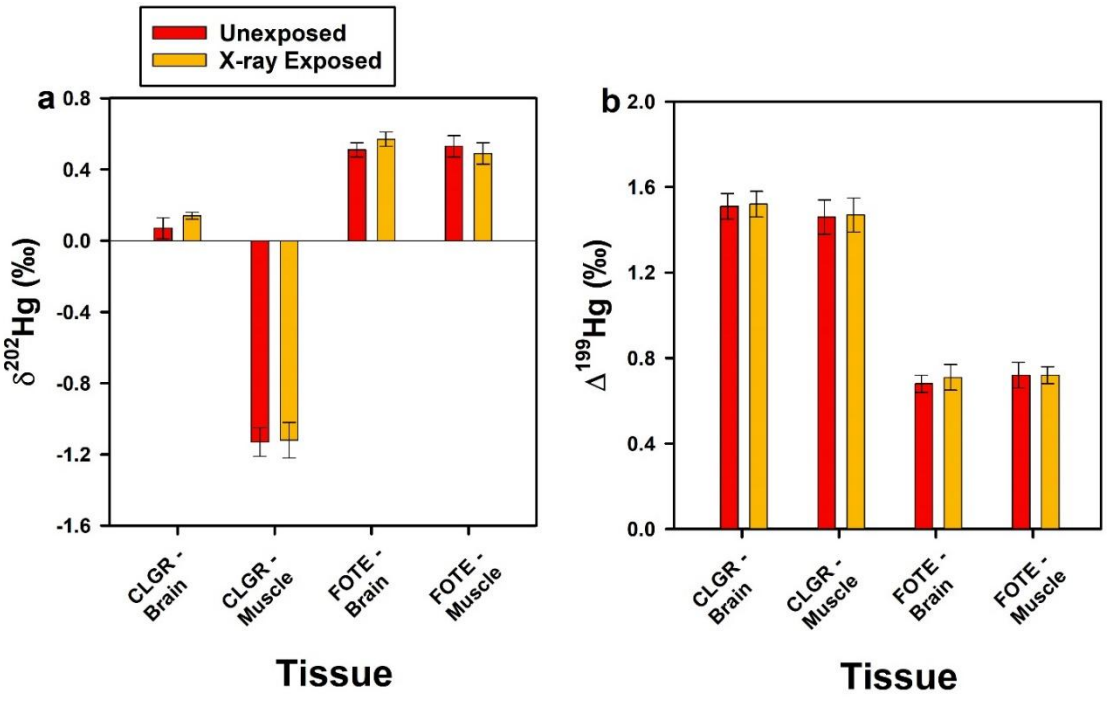

Figure S1. Stable mercury isotope ratios of (a) δ^{202}Hg and (b) Δ^{199}Hg of tissue samples that were analyzed unexposed (i.e., fresh) and previously exposed to the X-ray beam for HR-XANES measurements. Error bars present ±2SD. CLGR and FOTE stand for Clark's grebe and Forster's tern, respectively.

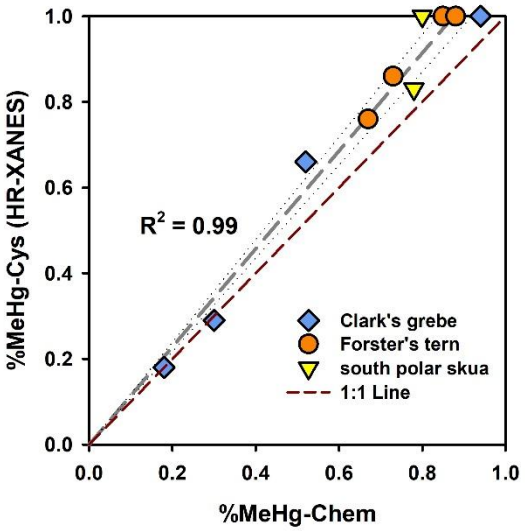

Figure S2. The linear relationship between the percentage of mercury quantified as methylmercury-cysteine determined by HR-XANES (%MeHg-Cys HR-XANES) and MeHg by chemical analysis (%MeHg-Chem) for bird tissues. The dashed gray line presents the fit of data, thin black lines the 95% confidence interval of the fit, and dark red line the 1:1 line.

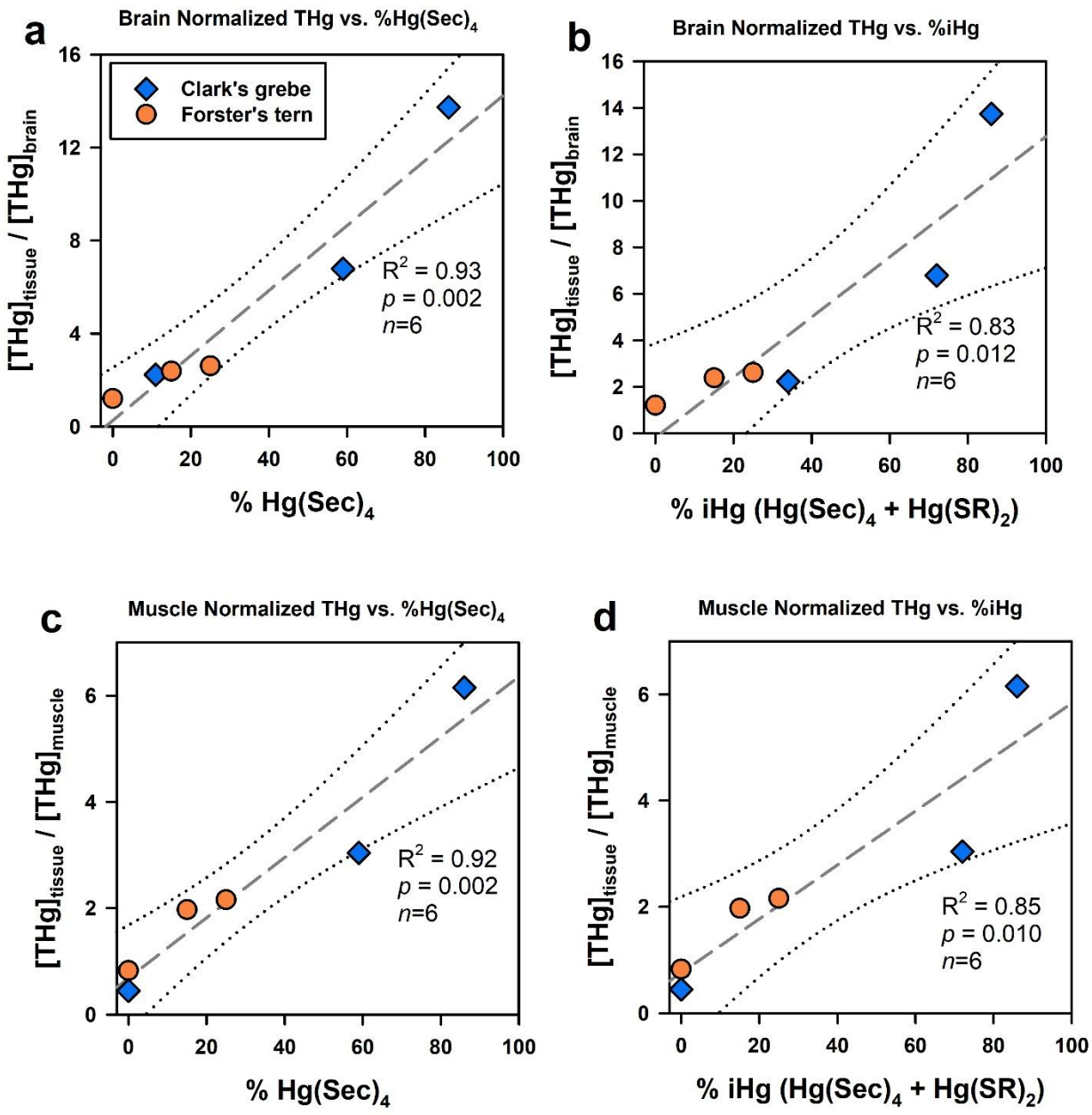

Figure S3. Total Hg concentration ratio between tissues ($[THg]_{tissue}$; tissues = muscle, kidneys, and liver) and the brain ($[THg]_{brain}$) as a function of (**a**) $\%Hg(Sec)_4$ and (**b**) %iHg ($Hg(Sec)_4$ + $Hg(SR)_2$) in the tissue. Total Hg concentration ratio between tissues ($[THg]_{tissue}$; tissues = brain, kidneys, and liver) and the muscle ($[THg]_{muscle}$) as a function of (**c**) $\%Hg(Sec)_4$ and (**d**) %iHg ($Hg(Sec)_4$ + $Hg(SR)_2$) in the tissue. The dashed gray lines present the linear fit of data and dotted black lines present the 95% confidence interval of the fit. Agreement in trends between plots the top panel (**a-b**, brain normalized) and bottom panel (**c-d**, muscle normalized) support the interpretation that iHg species help explain THg concentrations across tissues.

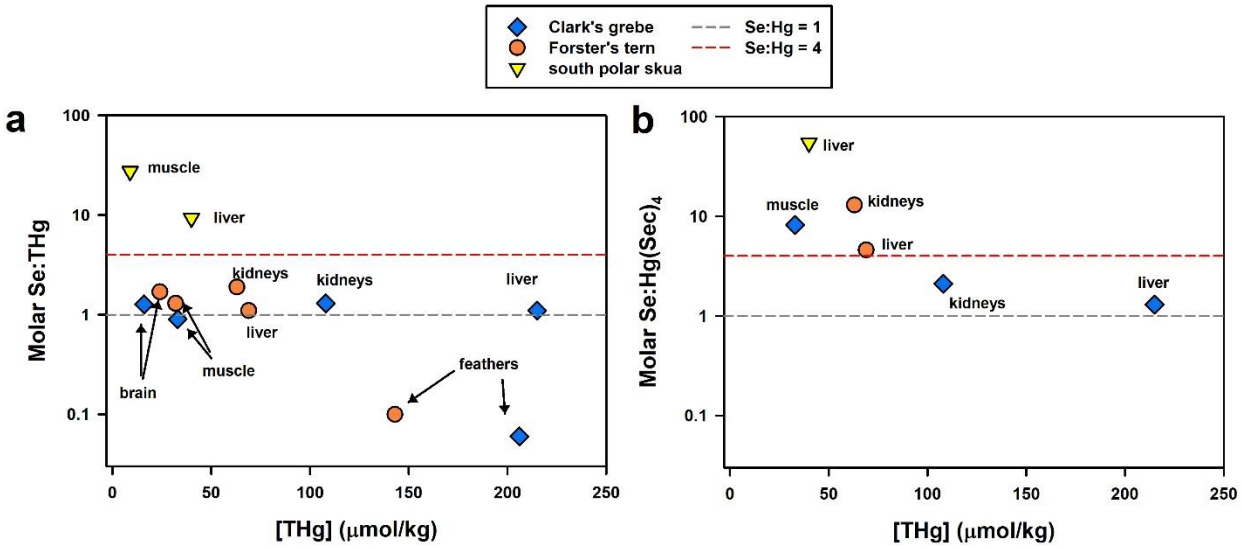

Figure S4. Molar ratios of (**a**) Se to total Hg (Se:THg) versus THg concentration and (**b**) Se to Hg as a tetraselenolate complex ($Se:Hg(Sec)_4$) versus THg concentration of the bird tissues and feathers. Horizontal dashed lines present stoichiometric ratios of 4 (red) and 1 (gray) for reference of ratios of $Hg(Sec)_4$ and HeSe species, respectively.

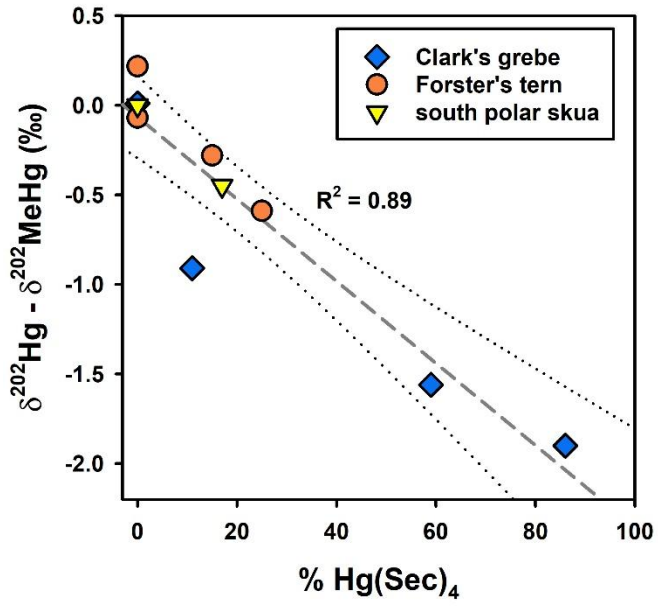

Figure S5. Relationship between the difference in $\delta^{202}Hg$ signatures of total mercury minus methylmercury ($\delta^{202}THg - \delta^{202}MeHg$) and the $\%Hg(Sec)_4$ as determined by HR-XANES spectroscopy (Table 1 in main text). The dashed gray and dotted black lines present the fit of data and 95% confidence interval of the fit, respectively.

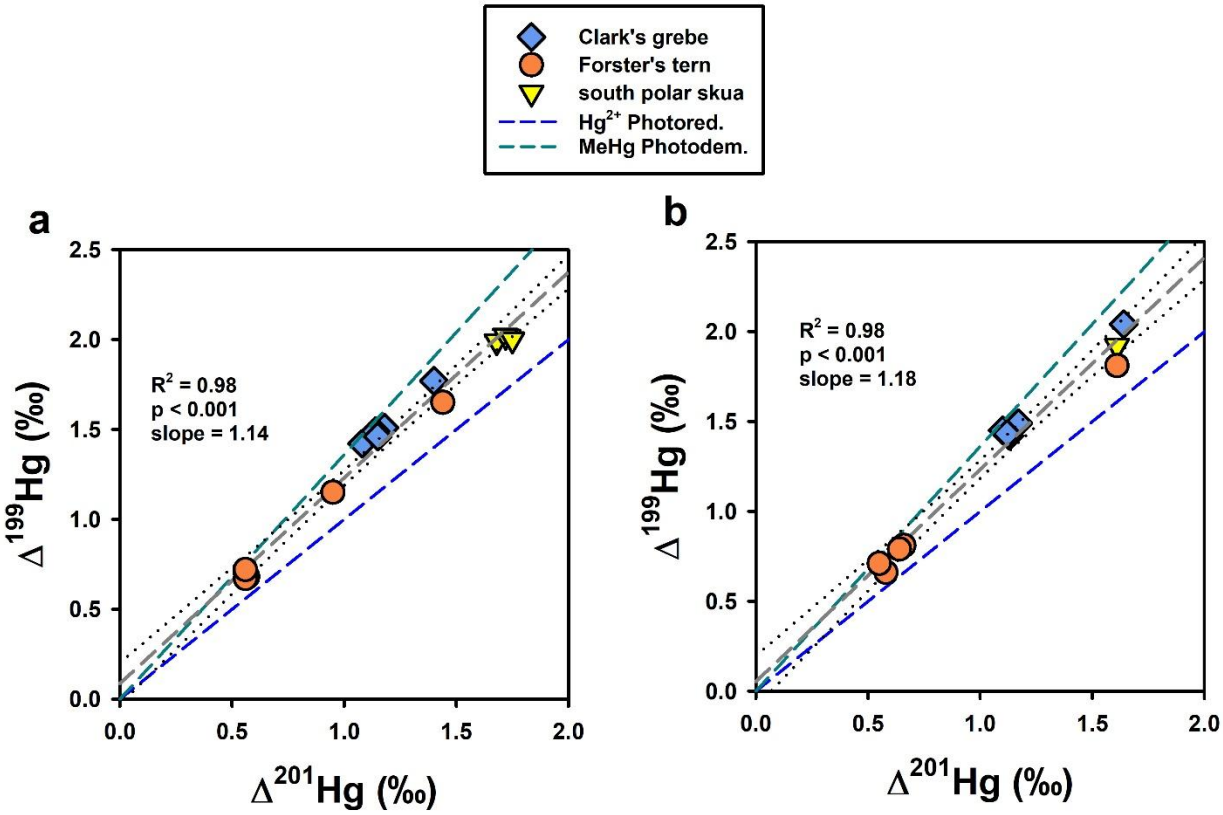

Figure S6. Odd mass-independent fractionation (MIF) isotope signatures (Δ^{199}Hg vs Δ^{201}Hg) of the (**a**) total mercury and (**b**) methylmercury (MeHg) of bird tissues and feathers. The dashed gray lines present the fit of data and black dotted lines the 95% confidence interval of the fit. Dashed blue and green lines present theoretical slopes for residual Hg(II) photoreduction and residual MeHg photodemethylation processes in water,[12] respectively.

Table S1. Mercury stable isotope ratios of certified reference materials (CRMs) and standards.

CRM	Fraction of Hg	δ^{199}Hg (±2SD)	δ^{200}Hg (±2SD)	δ^{201}Hg (±2SD)	δ^{202}Hg (±2SD)	δ^{204}Hg (±2SD)	Δ^{199}Hg (±2SD)	Δ^{200}Hg (±2SD)	Δ^{201}Hg (±2SD)	Δ^{204}Hg (±2SD)	*n*	Ref.
IAEA-407 , fish homogenate	THg	1.21 (0.04)	0.36 (0.05)	1.36 (0.08)	0.60 (0.04)	0.85 (0.07)	1.06 (0.03)	0.06 (0.06)	0.91 (0.07)	-0.04 (0.05)	3	Lepak et al. 2018,[13] Lepak et al. 2019[14]
DOLT-2, dogfish liver	MeHg	1.05 (0.09)	0.05 (0.06)	0.85 (0.11)	-0.04 (0.06)	-0.09 (0.08)	1.06 (0.07)	0.07 (0.03)	0.88 (0.06)	-0.04 (0.01)	2	Rosera et al. 2020[3]
UM Almadén (Secondary Isotope Standard)	THg and MeHg	-0.16 (0.06)	-0.27 (0.05)	-0.45 (0.07)	-0.55 (0.06)	-0.81 (0.11)	-0.02 (0.05)	0.01 (0.04)	-0.04 (0.05)	0.01 (0.10)	31	NIST , 2017

Table S2. Linear combination fit (LCF) results of HR-XANES spectra including the precision and quality of fit.

Tissue	%MeHg-Cys	%$Hg(Sec)_4$	%$Hg(SR)_2$	%Precision	NSS x 10^{5} [b]
Clark's grebe (*Aechmophorus clarkii*)[a]					
Brain	100	0	0	5	--
Muscle	66	11	23	5	1.1
Kidneys	28	59	12	5	1.9
Liver	14	86	0	5	2.4
Forster's tern (*Sterna forsteri*)					
Brain	100	0	0	--	--
Muscle	100	0	0	--	--
Kidneys	85	15	0	10	4.5
Liver	75	25	0	10	2.6
south polar skua (*Stercorarius maccormicki*)					
Muscle	100	0	0	10	--
Liver	83	17	0	10	2.2

[a] spectra and fit results are duplicated from Manceau et al. (2021).[1]

[b] NSS is the normalized sum-squared (Equation S3), a measure of the quality of fit.

Table S3. Isotope ratios of total mercury (THg) and methylmercury (MeHg) of the Clark's grebe and Forster's tern tissue samples and feathers.

Tissue	Fraction of Hg	δ^{199}Hg (±1SD)	δ^{200}Hg (±1SD)	δ^{201}Hg (±1SD)	δ^{202}Hg (±1SD)	δ^{204}Hg (±1SD)	Δ^{199}Hg (±1SD)	Δ^{200}Hg (±1SD)	Δ^{201}Hg (±1SD)	Δ^{204}Hg (±1SD)
Clark's grebe (*Aechmophorus clarkii*)										
Brain	THg[a]	1.53	0.07	1.23	0.07	0.04	1.51	0.03	1.18	-0.06
		(0.04)	(0.01)	(0.04)	(0.03)	(0.07)	(0.03)	(0.01)	(0.02)	(0.04)
	MeHg	1.51	0.02	1.21	0.06	0.11	1.49	-0.01	1.17	0.03
		(0.02)	(0.03)	(0.02)	(0.04)	(0.05)	(0.01)	(0.01)	(0.01)	(0.04)
Muscle	THg[a]	1.18	-0.55	0.30	-1.13	-1.73	1.46	0.02	1.15	-0.05
		(0.05)	(0.03)	(0.05)	(0.04)	(0.07)	(0.04)	(0.01)	(0.03)	(0.01)
	MeHg	1.38	-0.08	0.95	-0.22	-0.38	1.43	0.03	1.12	-0.04
		(0.02)	(0.01)	(0.01)	(0.03)	(0.07)	(0.02)	(0.02)	(0.01)	(0.04)
Kidneys	THg	1.07	-0.67	0.02	-1.41	-2.17	1.42	0.04	1.08	-0.06
		(0.05)	(0.01)	(0.04)	(0.03)	(0.07)	(0.04)	(0.01)	(0.02)	(0.03)
	MeHg[b]	1.49	0.11	1.20	0.14	0.21	1.45	0.04	1.10	0.00
		(0.02)	(0.03)	(0.02)	(0.02)	(0.02)	(0.03)	(0.02)	(0.01)	(0.02)
Liver	THg	0.97	-1.02	-0.42	-2.07	-3.17	1.49	0.02	1.14	-0.08
		(0.05)	(0.03)	(0.04)	(0.04)	(0.07)	(0.04)	(0.02)	(0.02)	(0.04)
	MeHg	1.37	-0.08	1.00	-0.17	-0.29	1.42	0.01	1.13	-0.04
		(0.02)	(0.02)	(0.03)	(0.02)	(0.03)	(0.02)	(0.01)	(0.03)	(0.02)
Breast Feather	THg	1.80	0.11	1.51	0.15	0.16	1.77	0.04	1.40	-0.06
		(0.02)	(0.01)	(0.01)	(0.03)	(0.05)	(0.02)	(0.01)	(0.02)	(0.02)
	MeHg	2.07	0.09	1.73	0.13	0.14	2.04	0.03	1.64	-0.05
		(0.03)	(0.01)	(0.05)	(0.05)	(0.08)	(0.03)	(0.01)	(0.03)	(0.06)
Forster's tern (*Sterna forsteri*)										
Brain	THg[a]	0.81	0.27	0.95	0.51	0.74	0.68	0.01	0.57	-0.01
		(0.03)	(0.01)	(0.01)	(0.02)	(0.04)	(0.02)	(0.01)	(0.02)	(0.02)
	MeHg	0.96	0.30	1.09	0.57	0.89	0.81	0.01	0.66	0.03
		(0.02)	(0.01)	(0.03)	(0.01)	(0.06)	(0.02)	(0.02)	(0.02)	(0.06)
Muscle	THg[a]	0.85	0.28	0.95	0.53	0.75	0.72	0.02	0.56	-0.03
		(0.03)	(0.01)	(0.02)	(0.03)	(0.04)	(0.03)	(0.01)	(0.03)	(0.05)
	MeHg	0.87	0.18	0.87	0.31	0.48	0.79	0.02	0.64	0.02
		(0.02)	(0.03)	(0.05)	(0.02)	(0.03)	(0.02)	(0.02)	(0.02)	(0.01)
Kidneys	THg	0.78	0.17	0.81	0.34	0.46	0.70	0.00	0.56	-0.05
		(0.03)	(0.01)	(0.02)	(0.02)	(0.03)	(0.03)	(0.01)	(0.01)	(0.02)
	MeHg	0.81	0.33	1.05	0.62	0.91	0.66	0.01	0.58	-0.02
		(0.03)	(0.01)	(0.01)	(0.03)	(0.02)	(0.02)	(0.02)	(0.01)	(0.06)
Liver	THg	0.64	-0.05	0.46	-0.14	-0.22	0.67	0.02	0.56	-0.02
		(0.04)	(0.01)	(0.01)	(0.02)	(0.03)	(0.03)	(0.01)	(0.03)	(0.04)
	MeHg[b]	0.82	0.26	0.89	0.45	0.68	0.71	0.03	0.55	0.01
		(0.08)	(0.03)	(0.05)	(0.04)	(0.09)	(0.08)	(0.03)	(0.04)	(0.04)
Breast Feather	THg	1.83	0.35	1.97	0.70	0.98	1.65	0.00	1.44	-0.06
		(0.04)	(0.02)	(0.01)	(0.03)	(0.04)	(0.04)	(0.01)	(0.03)	(0.05)
	MeHg	2.00	0.37	2.16	0.72	1.13	1.81	0.00	1.61	0.06
		(0.04)	(0.02)	(0.03)	(0.02)	(0.03)	(0.04)	(0.01)	(0.03)	(0.03)

[a]Identifies samples for which total Hg isotope ratios were measured on unexposed and X-ray exposed material.

[b]Identifies samples for which MeHg isotope ratios were measured in duplicate (CLGR Liver) and triplicate (FOTE Kidneys) chromatographic extracts.

Table S4. Isotope ratios of total mercury (THg) and methylmercury (MeHg) of the tissues of the south polar skua.

Tissue	Fraction of Hg	δ^{199}Hg (±1SD)	δ^{200}Hg (±1SD)	δ^{201}Hg (±1SD)	δ^{202}Hg (±1SD)	δ^{204}Hg (±1SD)	Δ^{199}Hg (±1SD)	Δ^{200}Hg (±1SD)	Δ^{201}Hg (±1SD)	Δ^{204}Hg (±1SD)
south polar skua (*Stercorarius maccormicki*)										
Muscle	THg	--	--	--	1.25 (0.05)	--	1.99 (0.03)	0.03 (0.03)	1.68 (0.05)	-0.02 (0.04)
	MeHg	--	--	--	--	--	--	--	--	--
Kidneys	THg	--	--	--	0.17 (0.03)	--	2.00 (0.05)	0.02 (0.06)	1.75 (0.03)	0.03 (0.03)
	MeHg	--	--	--	1.25 (0.01)	--	1.92 (0.02)	0.05 (0.01)	1.61 (0.03)	-0.03 (0.02)
Liver	THg	--	--	--	0.80 (0.01)	--	2.02 (0.04)	-0.02 (0.05)	1.72 (0.05)	-0.05 (0.05)
	MeHg	--	--	--	--	--	--	--	--	--

References

(1) Manceau, A.; Bourdineaud, J. P.; Oliveira, R. B.; Sarrazin, S. L. F.; Krabbenhoft, D. P.; Eagles-Smith, C. A.; Ackerman, J. T.; Stewart, A. R.; Ward-Deitrich, C.; del Castillo Busto, M. E.; Goenaga-Infante, H.; Wack, A.; Retegan, M.; Detlefs, B.; Glatzel, P.; Bustamante, P.; Nagy, K. L.; Poulin, B. A. Demethylation of methylmercury in bird, fish, and earthworm. *Environ. Sci. Technol.* **2021**, 55, 1527-1534, DOI: 10.1021/acs.est.0c04948.

(2) Kleckner, A. E.; Kakouros, E.; Robin Stewart, A. A practical method for the determination of total selenium in environmental samples using isotope dilution-hydride generation-inductively coupled plasma-mass spectrometry. *Limnol. Oceanogr. Methods* **2017**, *15*, 363–371, DOI: 10.1002/lom3.10164.

(3) Rosera, T. J.; Janssen, S. E.; Tate, M. T.; Lepak, R. F.; Ogorek, J. M.; DeWild, J. F.; Babiarz, C. L.; Krabbenhoft, D. P.; Hurley, J. P. Isolation of methylmercury using distillation and anion-exchange chromatography for isotopic analyses in natural matrices. *Anal. Bioanal. Chem.* **2020**, *412*, 681–690, DOI: 10.1007/s00216-019-02277-0.

(4) Janssen, S. E.; Lepak, R. F.; Tate, M. T.; Ogorek, J. M.; DeWild, J. F.; Babiarz, C. L.; Hurley, J. P.; Krabbenhoft, D. P. Rapid pre-concentration of mercury in solids and water for isotopic analysis. *Anal. Chim. Acta* **2019**, *1054*, 95-103, DOI: 10.1016/j.aca.2018.12.026.

(5) Yin, R.; Krabbenhoft, D. P.; Bergquist, B. A.; Zheng, W.; Lepak, R. F.; Hurley, J. P. Effects of mercury and thallium concentrations on high precision determination of mercury isotopic composition by Neptune Plus multiple collector inductively coupled plasma mass spectrometry. *J. Anal. At. Spectrom.* **2016**, *31, 2060-2068*, DOI: 10.1039/c6ja00107f.

(6) Rovezzi, M.; Lapras, C.; Manceau, A.; Glatzel, P.; Verbeni, R. High energy-resolution X-ray spectroscopy at ultra-high dilution with spherically bent crystal analyzers of 0.5 m radius. *Rev. Sci. Instrum.* **2017**, *88*, 013108, DOI: 10.1063/1.4974100.

(7) Manceau, A.; Bustamante, P.; Haouz, A.; Bourdineaud, J. P.; Gonzalez-Rey, M.; Lemouchi, C.; Gautier-Luneau, I.; Geertsen, V.; Barruet, E.; Rovezzi, M.; Glatzel, P.; Pin, S. Mercury(II) binding to metallothionein in *Mytilus Edulis* revealed by high energy-resolution XANES spectroscopy. *Chem. Eur. J.* **2019**, *25*, 997, DOI: 10.1002/chem.201804209.

(8) Manceau, A.; Gaillot, A. C.; Glatzel, P.; Cherel, Y; Bustamante, P. *In Vivo* formation of HgSe nanoparticles and Hg-tetraselenolate complex from methylmercury in seabird – Implications for the Hg-Se antagonism. *Environ. Sci. Technol.* **2021**, 55, 1515-1526, DOI: 10.1021/acs.est.0c06269.

(9) Mah, V.; Jalilehvand, F. Glutathione complex formation with mercury(II) in aqueous solution at physiological pH. *Chem. Res. Toxicol.* **2010**, *23*, 1815-1823, DOI: 10.1021/tx100260e.

(10) Manceau, A.; Wang, J.; Rovezzi, M.; Glatzel, P.; Feng, X. Biogenesis of mercury–sulfur nanoparticles in plant leaves from atmospheric gaseous Mmercury. *Environ. Sci. Technol.* **2018**, *52*, 3935–3948, DOI: 10.1021/acs.est.7b05452.

(11) Bourdineaud, J. P.; Gonzalez-Rey, M.; Rovezzi, M.; Glatzel, P.; Nagy, K. L.; Manceau, A. Divalent mercury in dissolved organic matter Is bioavailable to fish and accumulates as dithiolate and tetrathiolate complexes. *Environ. Sci. Technol.* **2019**, *53*, 4880-4891, DOI: 10.1021/acs.est.8b06579.

(12) Bergquist, B. A.; Blum, J. D. Mass-dependent and -independent fractionation of Hg isotopes by

photoreduction in aquatic systems. *Science* **2007**, *318*, 417-420, DOI: 10.1126/science.1148050.

(13) Lepak, R. F.; Janssen, S. E.; Yin, R.; Krabbenhoft, D. P.; Ogorek, J. M.; DeWild, J. F.; Tate, M. T.; Holsen, T. M.; Hurley, J. P. Factors affecting mercury stable isotopic distribution in piscivorous fish of the Laurentian Great Lakes. *Environ. Sci. Technol.* **2018**, *52*, 2768–2776. DOI: 10.1021/acs.est.7b06120.

(14) Lepak, R. F.; Hoffman, J. C.; Janssen, S. E.; Krabbenhoft, D. P.; Ogorek, J. M.; DeWild, J. F.; Tate, M. T.; Babiarz, C. L.; Yin, R.; Murphy, E. W.; Engstrom, D. R.; Hurley, J. P. Mercury source changes and food web shifts alter contamination signatures of predatory fish from Lake Michigan. *Proc. Natl. Acad. Sci. U. S. A.* **2019**, *116*, 23600-23608, DOI: 10.1073/pnas.1907484116.